

**Flavor composition of ultrahigh energy neutrinos at source and at neutrino telescopes**Sandhya Choubey<sup>1,\*</sup> and Werner Rodejohann<sup>2,†</sup><sup>1</sup>*Harish-Chandra Research Institute, Chhatnag Road, Jhansi, 211019 Allahabad, India*<sup>2</sup>*Max-Planck-Institut für Kernphysik, Postfach 103980, D-69029 Heidelberg, Germany*

(Received 1 October 2009; published 18 December 2009)

We parametrize the initial flux composition of high energy astrophysical neutrinos as  $(\Phi_e^0:\Phi_\mu^0:\Phi_\tau^0) = (1:n:0)$ , where  $n$  characterizes the source. All usually assumed neutrino sources appear as limits of this simple parametrization. We investigate how precise neutrino telescopes can pin down the value of  $n$ . We furthermore show that there is a neutrino mixing scenario in which the ratio of muon neutrinos to the other neutrinos takes a constant value *regardless of the initial flux composition*. This occurs when the muon neutrino survival probability takes its minimal allowed value. The phenomenological consequences of this very predictive neutrino mixing scenario are given.

DOI: 10.1103/PhysRevD.80.113006

PACS numbers: 14.60.Pq, 95.85.Ry

**I. INTRODUCTION**

Neutrino mass and mixing influences many phenomenological aspects of particle and astroparticle physics. In particular, any observed flavor mix of neutrinos  $\nu_e$ ,  $\nu_\mu$ , and  $\nu_\tau$  is usually not the original flavor mix, but rather a modified one. This is a consequence of the nontrivial structure of the leptonic mixing, or the Pontecorvo-Maki-Nakagawa-Saki (PMNS) mixing matrix. In this paper we wish to focus on the interplay of neutrino mixing and the flavor composition of ultrahigh energy (UHE) astrophysical neutrinos, whose detection is the goal of neutrino telescopes such as IceCube [1], currently under construction, or the planned KM3Net facility [2]. Many recent works discussed aspects of this problem [3–21], an overview can be found in [22].

The composition of the flux detectable in neutrino telescopes depends on two things—(i) the initial flavor composition at the source, and (ii) the standard (and possibly nonstandard) parameters of neutrino mixing. This means that there are two types of studies one may pursue with neutrino telescopes:

- (a) neutrino physics: the extraction of neutrino properties from measurements of flavor ratios;
- (b) astrophysics: the identification of the initial flavor composition of the flux of UHE neutrinos and using that to probe the type of source and its properties.

A large plethora of literature exists for item (a), where authors have studied the potential of probing the neutrino mixing angles using the flavor ratios. In this paper we will concentrate on item (b) and expound the potential of UHE neutrino measurements to decipher the flavor composition of the UHE neutrinos at their source (see Ref. [20] for related recent analyses). This could lead to a better understanding of the properties of the astrophysical source responsible for the production of these neutrinos. As will be

discussed in detail in Sec. III, different astrophysical situations could give rise to a variety of flavor ratios of the neutrinos. Since the usually assumed high energy neutrino sources do not generate tau neutrinos in any appreciable amounts, we neglect their presence in the initial UHE neutrino flux and propose a simple one parameter parametrization of the initial flux composition of the neutrinos:

$$(\Phi_e^0:\Phi_\mu^0:\Phi_\tau^0) = (1:n:0). \quad (1)$$

All discussed sources such as pion, muon-damped, charm, or neutron beams are simple limits of this parametrization. With such a parametrization the experimental determination of the initial flux composition is simply an extraction of the parameter  $n$  from the observed flux composition on Earth. We will define two kinds of measurable flux ratios and calculate the predicted values of these ratios at Earth for all values of  $n$  from  $0 - \infty$ , a range which covers all possible UHE neutrino flux sources. We show that the uncertainty on the predicted values of these flux ratios due to their dependence on the oscillation parameters threatens to wash out any sensitivity of the neutrino telescopes to  $n$ . We define a very simple  $\chi^2$  function and show quantitatively the ranges of  $n$  which could be ruled out by the data from UHE observations.

We also point out, for the first time, a special mixing scenario for which the observable ratio of muon neutrinos to the other neutrinos is independent of the initial mixing scenario. This occurs when the averaged survival probability for muon neutrinos takes its minimal allowed value of  $\frac{1}{3}$ . It illustrates nicely that the ratio of muon neutrinos with the other flavors alone may not be a good discriminator of different sources.

Our paper is built up as follows: in Sec. II we summarize the neutrino mixing phenomenology framework at neutrino telescopes. Section III sees the discussion of several neutrino sources whose common features lead to the parametrization in Eq. (1). The peculiar mixing scenario with a constant muon neutrino flux with respect to the total flux is presented in Sec. IV. The experimental determination of

\*sandhya@hri.res.in

†werner.rodejohann@mpi-hd.mpg.de

$n$  is investigated in Sec. V, before we sum up and conclude in Sec. VI.

## II. NEUTRINO MIXING AND NEUTRINO TELESCOPES

Astrophysical sources will generate fluxes of electron, muon and tau neutrinos, denoted by  $\Phi_e^0$ ,  $\Phi_\mu^0$ , and  $\Phi_\tau^0$ , respectively. As a consequence of nontrivial neutrino mixing, it is not this initial flux composition which arrives at terrestrial detectors. In fact, what is measurable is given by<sup>1</sup>

$$\begin{pmatrix} \Phi_e \\ \Phi_\mu \\ \Phi_\tau \end{pmatrix} = \begin{pmatrix} P_{ee} & P_{e\mu} & P_{e\tau} \\ P_{\mu e} & P_{\mu\mu} & P_{\mu\tau} \\ P_{\tau e} & P_{\tau\mu} & P_{\tau\tau} \end{pmatrix} \begin{pmatrix} \Phi_e^0 \\ \Phi_\mu^0 \\ \Phi_\tau^0 \end{pmatrix}, \quad (2)$$

where the neutrino mixing probability is

$$U = \begin{pmatrix} c_{12}c_{13} & s_{12}c_{13} & s_{13}e^{-i\delta} \\ -s_{12}c_{23} - c_{12}s_{23}s_{13}e^{i\delta} & c_{12}c_{23} - s_{12}s_{23}s_{13}e^{i\delta} & s_{23}c_{13} \\ s_{12}s_{23} - c_{12}c_{23}s_{13}e^{i\delta} & -c_{12}s_{23} - s_{12}c_{23}s_{13}e^{i\delta} & c_{23}c_{13} \end{pmatrix}, \quad (5)$$

where  $c_{ij} = \cos\theta_{ij}$ ,  $s_{ij} = \sin\theta_{ij}$ . The CP phase  $\delta$  is unknown. Because the traveled distance of the neutrinos is much larger than the oscillation length  $4\pi E/\Delta m^2$ , the mass-squared differences  $\Delta m^2$  drop out of the mixing probabilities. Furthermore, solar neutrino mixing is neither maximal, nor zero or  $\pi/2$ , and due to these reasons no transition probability  $P_{\alpha\beta}$  with  $\alpha \neq \beta$  is zero and no survival probability  $P_{\alpha\alpha}$  is one [11]. Consequently, high energy astrophysical neutrinos will always mix. To be precise, at  $1\sigma$  and  $3\sigma$  the entries of the flavor conversion matrix  $P_{\alpha\beta}$  are

$$P = \begin{cases} \begin{pmatrix} 0.529 \div 0.578 & 0.178 \div 0.296 & 0.158 \div 0.275 \\ \cdot & 0.341 \div 0.443 & 0.354 \div 0.394 \\ \cdot & \cdot & 0.354 \div 0.469 \end{pmatrix} & (\text{at } 1\sigma), \\ \begin{pmatrix} 0.486 \div 0.612 & 0.127 \div 0.344 & 0.118 \div 0.335 \\ \cdot & 0.333 \div 0.508 & 0.304 \div 0.403 \\ \cdot & \cdot & 0.333 \div 0.525 \end{pmatrix} & (\text{at } 3\sigma). \end{cases} \quad (6)$$

The consequences and phenomenology of the special values  $P_{\mu\mu} = 0.333$  and  $P_{\tau\tau} = 0.333$  will be dealt with in Sec. IV.

As is obvious from the ranges of the mixing parameters given above, a good zeroth order description of neutrino mixing is

$$U \simeq \begin{pmatrix} \cos\theta_{12} & \sin\theta_{12} & 0 \\ -\frac{\sin\theta_{12}}{\sqrt{2}} & \frac{\cos\theta_{12}}{\sqrt{2}} & -\frac{1}{\sqrt{2}} \\ -\frac{\sin\theta_{12}}{\sqrt{2}} & \frac{\cos\theta_{12}}{\sqrt{2}} & \frac{1}{\sqrt{2}} \end{pmatrix}. \quad (7)$$

Therefore, it proves, in particular, useful to expand in terms of

$$|U_{e3}| \quad \text{and} \quad \epsilon \equiv \frac{\pi}{4} - \theta_{23}. \quad (8)$$

<sup>1</sup>Everywhere in this paper we denote the fluxes at the source with a superscript 0 ( $\Phi^0$ ), while the observed fluxes will be denoted without any superscript.

$$P_{\alpha\beta} = P_{\beta\alpha} = \sum_i |U_{\alpha i}|^2 |U_{\beta i}|^2 \quad (3)$$

and  $U$  is the lepton mixing matrix. The current best-fit values as well as the allowed  $1\sigma$ ,  $2\sigma$ , and  $3\sigma$  ranges of the oscillation parameters are [23]

$$\begin{array}{ccc} \sin^2 \theta_{12} & \sin^2 \theta_{13} & \sin^2 \theta_{23} \\ 0.312 & 0.016 & 0.466 \\ 0.294 \div 0.331 & 0.006 \div 0.026 & 0.408 \div 0.539 \\ 0.278 \div 0.352 & 0.000 \div 0.036 & 0.366 \div 0.602 \\ 0.263 \div 0.375 & 0.000 \div 0.046 & 0.331 \div 0.644 \end{array} \quad (4)$$

These mixing angles can be related to elements of the PMNS mixing matrix via

Note that  $\frac{1}{2} - \sin^2\theta_{23} = \epsilon + \mathcal{O}(\epsilon^3)$ . The result of the expansion for the flavor mixing matrix is

$$\begin{aligned} P &\simeq \begin{pmatrix} 1-2c_{12}^2s_{12}^2 & c_{12}^2s_{12}^2 & c_{12}^2s_{12}^2 \\ \cdot & \frac{1}{2}(1-c_{12}^2s_{12}^2) & \frac{1}{2}(1-c_{12}^2s_{12}^2) \\ \cdot & \cdot & \frac{1}{2}(1-c_{12}^2s_{12}^2) \end{pmatrix} \\ &+ \Delta \begin{pmatrix} 0 & 1 & -1 \\ \cdot & -1 & 0 \\ \cdot & \cdot & 1 \end{pmatrix} + \frac{1}{2}\bar{\Delta}^2 \begin{pmatrix} 0 & 0 & 0 \\ \cdot & 1 & -1 \\ \cdot & \cdot & 1 \end{pmatrix} \\ &- \tilde{U}^2 \begin{pmatrix} 2 & -1 & -1 \\ \cdot & \frac{1}{2} & \frac{1}{2} \\ \cdot & \cdot & \frac{1}{2} \end{pmatrix}, \end{aligned} \quad (9)$$

where the universal first [8,11] and second [17,18] order correction terms are

$$\begin{aligned}\Delta &= \frac{1}{2}\sin^2 2\theta_{12}\epsilon + \frac{1}{4}\sin 4\theta_{12}\cos\delta|U_{e3}| \\ &\simeq \frac{1}{9}(\sqrt{2}\cos\delta|U_{e3}| + 4\epsilon), \\ \bar{\Delta}^2 &= 3\epsilon^2 + (\cos 2\theta_{12}\epsilon - \sin 2\theta_{12}\cos\delta|U_{e3}|)^2 \\ &\simeq 3\epsilon^2 + (2\sqrt{2}\cos\delta|U_{e3}| - \epsilon)^2.\end{aligned}\quad (10)$$

We have also given the expressions for the value  $\sin^2\theta_{12} = \frac{1}{3}$ . Note that  $\bar{\Delta}^2$  is positive semidefinite. The same holds for the third expansion parameter,

$$\tilde{U}^2 = (1 - 2c_{12}^2 s_{12}^2)|U_{e3}|^2 \simeq \frac{5}{9}|U_{e3}|^2, \quad (11)$$

which is usually only a subleading correction. The parameter  $\bar{\Delta}^2$  can seldomly be larger than the first order term  $\Delta$ . To be quantitative,

$$\begin{aligned}\text{at } 1\sigma: & -0.046 \leq \Delta \leq 0.069, & \bar{\Delta}^2 \leq 0.060, \\ & 0.003 \leq \tilde{U}^2 \leq 0.015, \\ \text{at } 3\sigma: & -0.101 \leq \Delta \leq 0.112, & \bar{\Delta}^2 \leq 0.162, \\ & \tilde{U}^2 \leq 0.028.\end{aligned}\quad (12)$$

The dependence of the expansion parameters on  $\theta_{12}$  is weak. From the expressions for  $\Delta$  and  $\bar{\Delta}^2$ , it is clear that their dependence on the atmospheric neutrino mixing angle  $\theta_{23}$  is stronger than the one on  $|U_{e3}|\cos\delta$  [19].

### III. INITIAL FLUX COMPOSITIONS AND THEIR PARAMETRIZATION

We now turn to the observable flavor ratios [24,25]. The most frequently considered and experimentally most accessible is the ratio of flux of muon neutrinos to that of all other flavors:

$$T = \frac{\Phi_\mu}{\Phi_e + \Phi_\mu + \Phi_\tau} = \frac{\Phi_\mu}{\Phi_{\text{tot}}}. \quad (13)$$

Often one considers also the ratio  $\Phi_\mu/(\Phi_e + \Phi_\tau)$ , which is simply  $T/(1-T)$ . Whereas muon neutrinos with their characteristic tracks (continuous loss of energy via Cerenkov radiation) can be somewhat easily distinguished from electron and tau neutrinos, the distinction of the latter two is more difficult. If possible (e.g., via electromagnetic vs hadronic showers, or tau-induced lollipop/double bang events), one may consider their ratio as well:

$$R = \frac{\Phi_e}{\Phi_\tau}. \quad (14)$$

We will use these ratios  $T$  and  $R$  in this paper. When neutrinos and antineutrinos are not distinguished, then two independent ratios are sufficient to fully determine the flavor content. For instance, if both  $T$  and  $R$  are known, the ratio of muon neutrinos to tau neutrinos  $S$  is related to  $T$  and  $R$  via  $T = S/(S + R + 1)$ .

In what regards initial flux compositions, typically one considers pionic beam-dump-like sources, which have an

initial flux composition of

$$(\Phi_e^0:\Phi_\mu^0:\Phi_\tau^0) = (1:2:0). \quad (15)$$

They arise because hadronic processes in a cosmic ray source produce pions. If the medium in such a source is opaque to muons, then one speaks of muon-damped cases [26], which have a composition of

$$(\Phi_e^0:\Phi_\mu^0:\Phi_\tau^0) = (0:1:0). \quad (16)$$

Another possibility are so-called neutron beams, which result when photodisintegration creates neutrons from nuclei [27], and therefore

$$(\Phi_e^0:\Phi_\mu^0:\Phi_\tau^0) = (1:0:0). \quad (17)$$

Finally, at high energies semileptonic decays of charm quarks<sup>2</sup> may generate an initial flavor ratio of [28]

$$(\Phi_e^0:\Phi_\mu^0:\Phi_\tau^0) = (1:1:0). \quad (18)$$

We see that in all sources no tau neutrinos are generated initially. There is in fact always a small component (“prompt  $\nu_\tau$ ”) from decays such as  $D_s \rightarrow \tau\nu_\tau$ , however this contribution is at most at the permille level and can safely be neglected. We stress however that all of the above sources can be expected to be “impure,” i.e., there will be small deviations from the idealized compositions given above [9,13,18]. As one example, Ref. [13] has argued that because of the wrong helicity polarization of the muons in pion decay the  $\nu_\mu$  have actually a softer spectrum, and thus the effective count of muon neutrinos is reduced. This depends on the injection spectrum, which is described by the power law  $E^{-\alpha}$ . For the canonical value  $\alpha = 2$  it was found that effectively  $(\Phi_e^0:\Phi_\mu^0:\Phi_\tau^0) = (1:1.86:0)$ . It was shown [18] that inclusion of leptonic and semileptonic kaon decays, as well as of heavy flavor decays, does not change this ratio appreciably.

One may also consider Greisen-Zatsepin-Kuzmin neutrinos [29], whose flavor content changes with energy. Below about 100 PeV ( $10^8$  GeV), one has (1:0:0), whereas for higher energies (1:2:0).

Given all the above discussion, we are lead to parametrize the initial flux composition of high energy neutrinos simply as

$$(\Phi_e^0:\Phi_\mu^0:\Phi_\tau^0) = (1:n:0). \quad (19)$$

The experimental determination of the initial flux composition is therefore simply an extraction of the parameter  $n$  from the observed flux composition on Earth.<sup>3</sup> From Eq. (19) one can obtain (pure) pion sources when  $n = 2$ , neutron beams for  $n = 0$ , charm sources for  $n = 1$ , and muon-damped sources when one takes the limit  $n \rightarrow \infty$ .

<sup>2</sup>For bottom quark decays the production rate is suppressed by 1 order of magnitude.

<sup>3</sup>Reference [6] has proposed  $(\Phi_e^0:\Phi_\mu^0:\Phi_\tau^0) = (\sin^2\xi\cos^2\zeta:\cos^2\xi\cos^2\zeta:\sin^2\zeta)$ .

Let us attempt to express the flux ratios  $T$  and  $R$  in a source-independent way. We take advantage of the parametrization in Eq. (19) and use the expansion of the probabilities  $P_{\alpha\beta}$  in Eq. (9). First we consider the ratio of muon to all neutrinos and find

$$T = \frac{\Phi_\mu}{\Phi_{\text{tot}}} = \frac{P_{e\mu} + nP_{\mu\mu}}{1+n} \approx \frac{1}{1+n} \left[ \frac{n}{2} + \left(1 - \frac{n}{2}\right) c_{12}^2 s_{12}^2 + \Delta(1-n) + \frac{n}{2} \bar{\Delta}^2 + \tilde{U}^2 \left(1 - \frac{n}{2}\right) \right]. \quad (20)$$

We note the following points from this expression:

- (i) For  $n = 2$ , which corresponds to pionic sources, there is no explicit dependence on  $\theta_{12}$  and also corrections due to  $\tilde{U}^2$  vanish. The uncertainty on  $T$  is hence expected to be amongst the lowest for this case.
- (ii) For  $n = 1$ , which corresponds to charm sources, there is no first order correction  $\Delta$ , and thus corrections to the zeroth order expression are only of quadratic order in the small expansion parameters  $\theta_{23} - \pi/4$  and  $|U_{e3}|$ .

In the zeroth order approximation, which corresponds to  $\mu$ - $\tau$  symmetry yielding  $\theta_{13} = 0$  and  $\theta_{23} = 0$  such that the correction terms  $\Delta$ ,  $\bar{\Delta}$ , and  $\tilde{U}$  are all vanishing, Eq. (20) reduces to

$$T = \frac{1}{1+n} \left[ \frac{n}{2} + \left(1 - \frac{n}{2}\right) c_{12}^2 s_{12}^2 \right] \rightarrow \begin{cases} \frac{1}{3} & \text{for } n = 2 \text{ (pion source)} \\ \frac{1}{4} (1 + c_{12}^2 s_{12}^2) \approx \frac{11}{36} & \text{for } n = 1 \text{ (charm source)} \\ c_{12}^2 s_{12}^2 \approx \frac{2}{9} & \text{for } n = 0 \text{ (neutron beam)} \\ \frac{1}{2} (1 - c_{12}^2 s_{12}^2) \approx \frac{7}{18} & \text{for } n = \infty \text{ (muon damped),} \end{cases}$$

where we have also given the simple expressions for the special values of  $n$  corresponding to the usual sources one considers. Hence, we note that all sources have similar predicted  $T$  around 0.3. Indeed, in Sec. IV we will present an extreme scenario in which  $T = \frac{1}{3}$  independent of  $n$ . We further note that the predicted  $T$  is highest for  $n = \infty$ , lowest for  $n = 0$ , and intermediate for  $n = 1$  and 2. In general,  $T$  slightly increases with  $n$ .

Similarly, the ratio  $R$  of electron and tau neutrinos is

$$R = \frac{\Phi_e}{\Phi_\tau} = \frac{P_{ee} + nP_{e\mu}}{P_{e\tau} + nP_{\mu\tau}} = \frac{1 - 2c_{12}^2 s_{12}^2 (1 - \frac{n}{2}) + n\Delta - 2\tilde{U}^2 (1 - \frac{n}{2})}{\frac{n}{2} + c_{12}^2 s_{12}^2 (1 - \frac{n}{2}) - \Delta - \frac{n}{2} \bar{\Delta}^2 + \tilde{U}^2 (1 - \frac{n}{2})}. \quad (21)$$

Here the value  $n = 2$  removes again several correction terms, in particular, the terms with explicit dependence on  $\theta_{12}$ , which leads to small uncertainty. For the case of  $\mu$ - $\tau$  symmetry, one finds

$$R = \frac{1 - 2c_{12}^2 s_{12}^2}{\frac{n}{2} + c_{12}^2 s_{12}^2 (1 - \frac{n}{2})} \rightarrow \begin{cases} 1 & \text{for } n = 2 \text{ (pion source)} \\ 2 \frac{1 - c_{12}^2 s_{12}^2}{1 - c_{12}^2 s_{12}^2} \approx \frac{14}{11} & \text{for } n = 1 \text{ (charm source)} \\ \frac{1 - 2c_{12}^2 s_{12}^2}{c_{12}^2 s_{12}^2} \approx \frac{5}{2} & \text{for } n = 0 \text{ (neutron beam)} \\ 2 \frac{c_{12}^2 s_{12}^2}{1 - c_{12}^2 s_{12}^2} \approx \frac{4}{7} & \text{for } n = \infty \text{ (muon damped).} \end{cases}$$

The spread for the different values of  $n$  is larger than for  $T$ . For instance, if  $n = 2$  then  $R = 1$  at leading order and between  $0.820 \div 1.450$  for the  $3\sigma$  range, while  $n = 1$  leads to  $R = \frac{14}{11}$  at leading order and between  $0.998 \div 1.853$  for the  $3\sigma$  range. In general,  $R$  slightly decreases with  $n$ .

In Fig. 1 we show  $T$  and  $R$  as a function of  $n$ . In Table I we present the  $1\sigma$  and  $3\sigma$  ranges of predicted  $T$  and  $R$  for the four benchmark cases of  $n$  corresponding to pion, charm, neutron, and muon-damped sources. The  $1\sigma$  and  $3\sigma$  ranges of  $T$  and  $R$  correspond to current  $1\sigma$  and  $3\sigma$

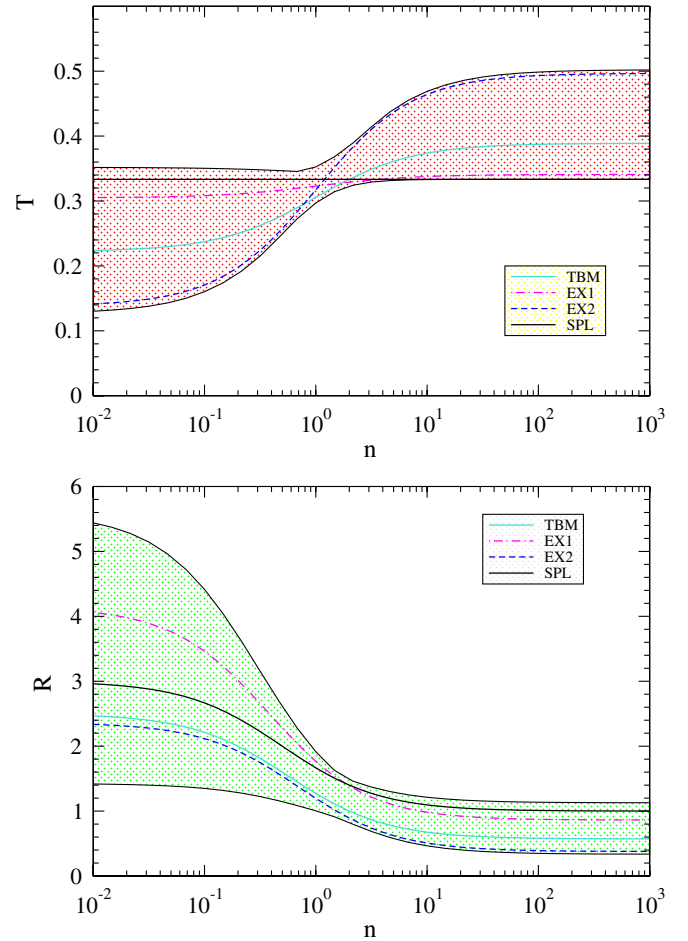


FIG. 1 (color online). Range of allowed values of  $T = \Phi_\mu/\Phi_{\text{tot}}$  (upper plot) and  $R = \Phi_e/\Phi_\tau$  (lower plot) as a function of the flux composition parameter  $n$ , when the oscillation parameters are varied within their  $3\sigma$  ranges.

TABLE I. Ranges of the flux ratios  $T = \Phi_\mu/\Phi_{\text{tot}}$  and  $R = \Phi_e/\Phi_\tau$  for an initial flux composition of  $(\Phi_e^0:\Phi_\mu^0:\Phi_\tau^0) = (1:n:0)$ . The case  $n = 2$  corresponds to pion sources,  $n = 1$  to charm sources,  $n = 0$  to neutron beams, and  $n \rightarrow \infty$  to muon-damped sources. We have inserted the  $1\sigma$  and  $3\sigma$  ranges of the oscillation parameters.

	$n$	$T$		$R$	
		$1\sigma$	$3\sigma$	$1\sigma$	$3\sigma$
Pion	2	0.324 ÷ 0.355	0.323 ÷ 0.387	0.893 ÷ 1.247	0.820 ÷ 1.450
Charm	1	0.303 ÷ 0.323	0.298 ÷ 0.348	1.121 ÷ 1.581	0.998 ÷ 1.853
Neutron	0	0.178 ÷ 0.296	0.127 ÷ 0.345	1.922 ÷ 3.618	1.449 ÷ 5.090
Muon-damped	$\infty$	0.341 ÷ 0.443	0.333 ÷ 0.508	0.462 ÷ 0.814	0.344 ÷ 1.071

ranges of the oscillation parameters. In general, one notes again that  $T$  is not an ideal discriminator in order to distinguish the neutrino source, because it is rather close to  $\frac{1}{3}$  for all  $n$ . Therefore, at the present stage we can already suspect that the task of identifying  $n$  will be easier when  $R$  is added to the statistics. A more detailed analysis will be presented in Sec. V.

#### IV. AN EXTREME CASE: MINIMAL SURVIVAL PROBABILITIES

One observes from the allowed ranges of the oscillation probabilities in Eq. (6) that  $P_{\mu\mu}$  and  $P_{\tau\tau}$  can take the value 0.333 when the  $3\sigma$  ranges of the oscillation parameters are inserted. It is worth noting that  $\frac{1}{3}$  is the minimal value that an averaged survival probability  $P_{\alpha\alpha}$  can take if there are three fermion families. In general, in the presence of  $k$  flavors we have

$$P_{\alpha\alpha}^{\text{min}} = \frac{1}{k}. \quad (22)$$

The minimum is obtained if and only if  $|U_{\alpha i}|^2 = 1/k$  for all  $i$ , i.e., when all mixing matrix elements of a row take on the same value.<sup>4</sup>

Considering the case of  $k = 3$ , let us discuss first the phenomenological consequences of  $|U_{\mu i}| = \sqrt{1/3}$ . The case of  $|U_{\tau i}| = \sqrt{1/3}$  will be discussed at the end of this section. First we note that unitarity of the PMNS matrix links the three entries of a row, which implies that only two independent constraints can result. The first one stems from  $|U_{\mu 3}| = \sqrt{1/3}$  and is

$$\sin^2\theta_{23} = \frac{1}{3} \frac{1}{1 - |U_{e3}|^2} \approx \frac{1}{3} (1 + |U_{e3}|^2). \quad (23)$$

Inserting this in  $|U_{\mu 1}| = \sqrt{1/3}$  gives the second independent constraint:

<sup>4</sup>Note that this concerns the elements of a *row*. Commonly it is assumed the elements of a *column* are identical (as for tribimaximal, or more general trimaximal mixing [30]).

$$\cos\delta \tan 2\theta_{12} = \frac{1 - 2|U_{e3}|^2}{|U_{e3}|\sqrt{2 - 3|U_{e3}|^2}} \approx \frac{1}{\sqrt{2}} \left( \frac{1}{|U_{e3}|} + \frac{5}{4}|U_{e3}| \right). \quad (24)$$

We immediately see that  $|U_{e3}|$  should be rather large,  $\sin^2\theta_{23}$  significantly less than  $\frac{1}{2}$ , and  $\cos\delta$  should be different from zero, or  $\sin\delta$  different from 1. We display the phenomenology resulting from Eqs. (23) and (24) in Fig. 2. While  $\sin^2\theta_{23}$  lies close to its lower  $3\sigma$  bound,  $\sin^2\theta_{12}$  can approach its upper  $1\sigma$  bound from above, in which case  $|U_{e3}|$  is close to its current upper bound and  $\delta$  less than one (or larger than 5). Vanishing  $\theta_{13}$  leads to maximal  $\theta_{12}$  and is disallowed.

The condition  $|U_{\mu i}|^2 = \frac{1}{3}$  together with unitarity of the PMNS matrix fix the form of the matrix  $|U_{\alpha i}|^2$ , namely,

$$|U_{\alpha i}|^2 = \begin{pmatrix} |U_{e1}|^2 & 1 - |U_{e1}|^2 - |U_{e3}|^2 & |U_{e3}|^2 \\ \frac{2}{3} - \frac{1}{3}|U_{e1}|^2 & |U_{e1}|^2 + |U_{e3}|^2 - \frac{1}{3} & \frac{2}{3} - \frac{1}{3}|U_{e3}|^2 \end{pmatrix}. \quad (25)$$

Recall that the  $|U_{\alpha i}|^2$ , and therefore the averaged probabilities  $P_{\alpha\beta}$ , depend on four independent parameters. The condition  $|U_{\mu i}| = \sqrt{1/3}$  fixes two of the four parameters and we have chosen  $|U_{e1}|^2$  and  $|U_{e3}|^2$  as the remaining two free and independent parameters. It is easy to see that from Eq. (25) the relation

$$P_{\mu\alpha} = P_{\alpha\mu} = \frac{1}{3} \quad \text{for } \alpha = e, \mu, \tau \quad (26)$$

follows. With this relation, one obtains a remarkably simple result for the ratio  $T$  as a function of  $n$ , namely,

$$T = \frac{\Phi_\mu}{\Phi_{\text{tot}}} = \frac{P_{e\mu} + nP_{\mu\mu}}{1 + n} = \frac{1}{3}, \quad (27)$$

regardless of  $n$ . The origin of this simple result is of course that all neutrinos  $\nu_i$  have an equal share in  $\nu_\mu$ , i.e., their muon content is equally distributed.<sup>5</sup> Concerning  $R$ , the general result as a function of  $n$  is rather lengthy. The allowed ranges of  $R$  are however significantly less than for the unconstrained case. For instance,  $R$  for pion sources

<sup>5</sup>Similarly, the ratio of muon neutrinos to the sum of electron and tau neutrinos is  $\Phi_\mu/(\Phi_e + \Phi_\tau) = \frac{1}{2}$ .



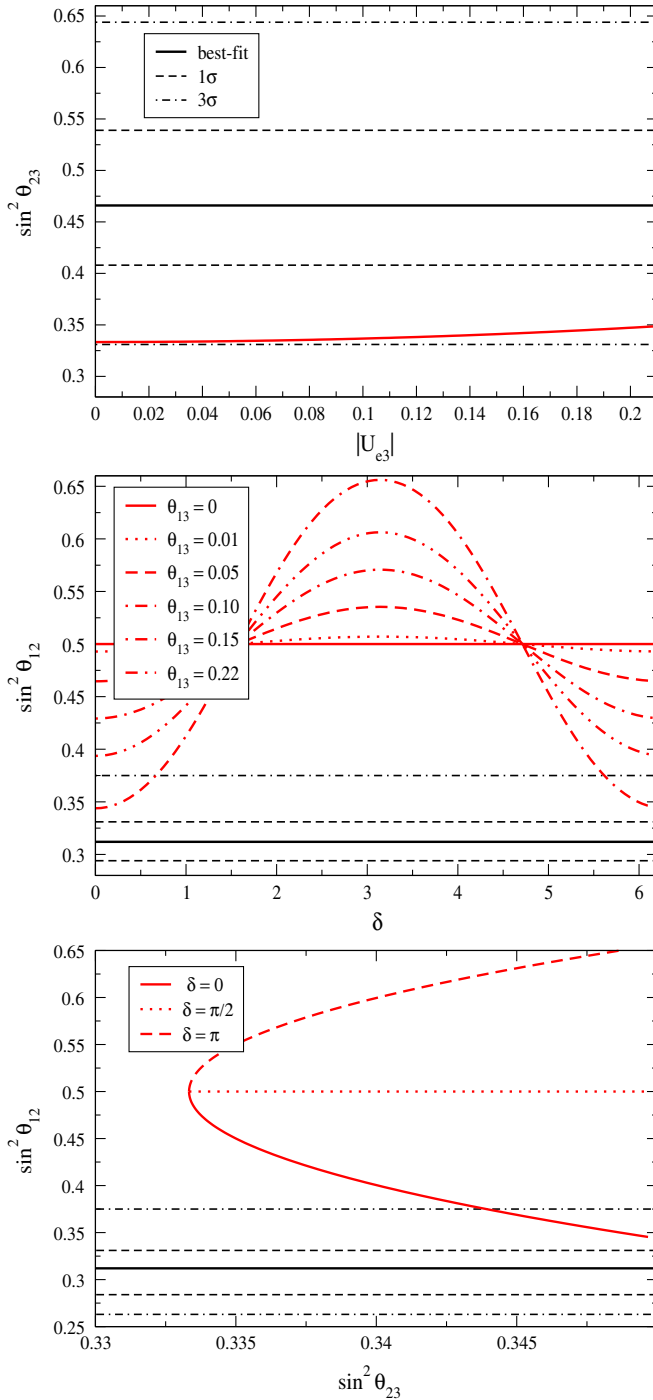


FIG. 2 (color online). Phenomenology of a PMNS matrix with all elements of the second row equal to each other. Shown are the atmospheric neutrino parameter  $\sin^2\theta_{23}$  against  $|U_{e3}|$ , the solar neutrino parameter  $\sin^2\theta_{12}$  against  $\delta$  for different values of  $|U_{e3}|$ , and  $\sin^2\theta_{12}$  against  $\sin^2\theta_{23}$ . Also given are the current best-fit value and the  $1\sigma$  as well as  $3\sigma$  ranges of the oscillation parameters.

lies between 1.23 and 1.40, to be compared with the general allowed range between 0.82 and 1.45. An interesting case occurs for muon-damped sources, for which we find that  $R = 1$ .

If the third row of  $U$  has identical entries, and therefore  $P_{\tau\tau} = \frac{1}{3}$ , then

$$\sin^2\theta_{23} = \frac{1}{3} \frac{1}{1 - |U_{e3}|^2} (2 - 3|U_{e3}|^2) \simeq \frac{2}{3} \left(1 - \frac{1}{2}|U_{e3}|^2\right) \quad (28)$$

and

$$\begin{aligned} \cos\delta \tan 2\theta_{12} &= -\frac{1 - 2|U_{e3}|^2}{|U_{e3}| \sqrt{2 - 3|U_{e3}|^2}} \\ &\simeq \frac{-1}{\sqrt{2}} \left( \frac{1}{|U_{e3}|} - \frac{5}{4}|U_{e3}| \right). \end{aligned} \quad (29)$$

While the second constraint is very similar to the one for  $|U_{\mu i}|^2 = \frac{1}{3}$ , the first condition implies here that  $\sin^2\theta_{23}$  lies slightly outside its allowed  $3\sigma$  range. The value  $P_{\tau\tau}^{\min} = 0.333$  found in Eq. (6) is therefore only numerically close to  $\frac{1}{3}$ . In any case, since the identification of muon neutrinos is much simpler than of tau neutrinos, it makes little sense to discuss the scenario with a saturated  $P_{\tau\tau}^{\min}$ .

## V. EXPERIMENTAL DISTINCTION OF SOURCES

In this section we explore the potential of the neutrino telescopes to ascertain the initial flux composition at the source. We stress that all results to be shown have been obtained by an exact calculation of the oscillation probabilities. We begin by returning to Fig. 1, in which we display the current  $3\sigma$  predicted ranges of  $T$  and  $R$  respectively, as a function of the flux composition parameter  $n$ . For each value of  $n$ , we calculated the full range of predicted values of  $T$  and  $R$  by allowing the oscillation parameters to vary in their current  $3\sigma$  allowed range [23]. The range of values of  $T$  and  $R$  for the different limiting cases is given in Table I. As discussed before, we note from the figure that the  $T$  ranges for all  $n$  are overlapping. We also note that the spread in  $T$  is minimized for values of  $n$  close to 2, as for this case the explicit dependence on  $\theta_{12}$  vanishes [cf. Eq. (20)]. For the same reason, the spread in  $R$  is also minimized for values of  $n$  close to 2 [cf. Eq. (21)]. The spread in  $T$  for small  $n$  is somewhat larger than for large  $n$ . The spread in  $R$  for small  $n$  is seen to be significantly larger than for large  $n$ . The large spread for small  $n$  of both  $T$  and  $R$  implies that neutron sources have the largest dependence on the neutrino mixing parameters. Note that, while the possible spread induced by neutrino mixing is smallest for  $n$  between 1 and 2, it does not necessarily imply that the sensitivity to initial flux composition will be best for these cases. We also note that  $R$  appears to be a much better discriminator for  $n$  compared to  $T$  and hence inclusion of  $R$  in addition to  $T$  will make the identification of the source easier. The individual lines embedded in the band in Fig. 1 show the predicted  $T$  and  $R$  for several benchmark mixing scenarios, in which the values of the oscillation parameters are

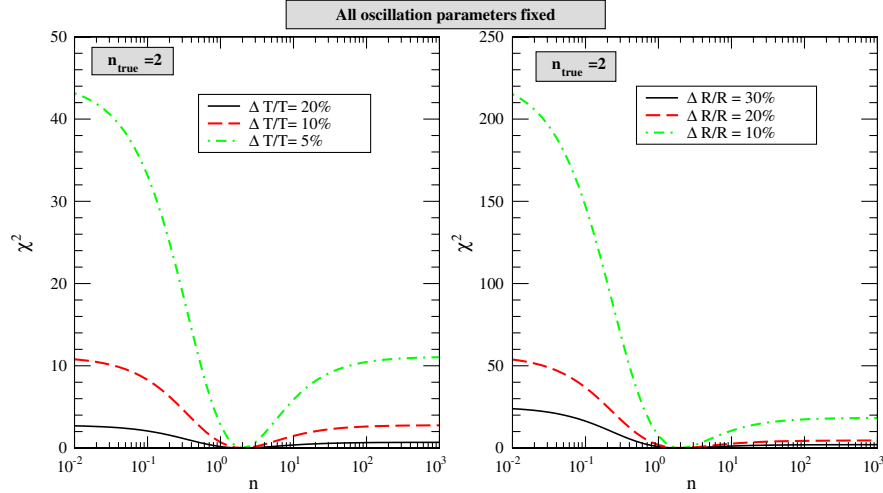


FIG. 3 (color online).  $\chi^2$  as a function of  $n_{\text{fit}}$  for  $n_{\text{true}} = 2$ , for different values of errors on the flux ratios  $T$  (left panel) and  $R$  (right panel). All oscillation parameters are fixed in the fit.

“TBM” the tribimaximal scenario: the oscillation parameters are  $\sin^2\theta_{12} = \frac{1}{3}$ ,  $\sin^2\theta_{23} = \frac{1}{2}$ ,  $|U_{e3}|^2 = 0$ , and  $\delta = 0$ ;

“EX1” extreme scenario 1: the oscillation parameters are  $\sin^2\theta_{12} = 0.27$ ,  $\sin^2\theta_{23} = 0.35$ ,  $|U_{e3}|^2 = 0.04$ , and  $\delta = 0$ ;

“EX2” extreme scenario 2: the oscillation parameters are  $\sin^2\theta_{12} = 0.27$ ,  $\sin^2\theta_{23} = 0.65$ ,  $|U_{e3}|^2 = 0.0$ , and  $\delta = 0$ ;

“SPL” special scenario: for the special scenario discussed in the previous section, we take  $\sin^2\theta_{12} = 0.352$ ,  $\sin^2\theta_{23} = 0.348$ ,  $|U_{e3}|^2 = 0.043$ , and  $\delta = 0$ .

One can immediately see from Fig. 1 that as predicted in Sec. IV, the special case yields  $T = 1/3$  for all values of  $n$ . Therefore, if this case was the true mixing scenario chosen by Nature, then it would be impossible to conclude anything about  $n$  from  $T$  measurement at neutrino telescopes. One can also note that  $T$  for the EX1 mixing case is very close to the SPL case and, hence, it would also be difficult to say anything about the source, if this set of mixing parameters turns out to be the true mixing angles.

We next define a very simple  $\chi^2$  function as<sup>6</sup>

$$\chi^2 = \left( \frac{F_{\text{data}} - F_{\text{theory}}}{\sigma_F} \right)^2, \quad (30)$$

where  $F$  can be either  $T$  or  $R$  and “data” and “theory” refer to observed and predicted flux ratios respectively, and  $\sigma_F$  is the  $1\sigma$  experimental error on the relevant flux ratio. We show results for fixed experimental errors of 20%, 10%, and 5% for  $T$  and 30%, 20%, and 10% for  $R$ . We

<sup>6</sup>We are aware that this definition of  $\chi^2$  is not strictly valid for a ratio as its error will not be Gaussian. Nonetheless we use it here for the sake of simplicity as the purpose of this paper is to roughly illustrate the potential of the neutrino telescope rather than to show exact numerical results for which one should work with the actual number of events calculated using a detailed code for the detector including threshold, efficiencies, and so on.

generate the “ $F_{\text{data}}$ ” at certain “true” values  $n$ , denoted as  $n_{\text{true}}$ , and at one of the benchmark mixing scenarios given above. This  $F_{\text{data}}$  is then fitted with  $F_{\text{theory}}$  corresponding to  $n_{\text{fit}}$ . The oscillation parameters in the fit are generally allowed to vary freely in the fit, apart from Fig. 3.

In Fig. 3 we show the  $\chi^2$  obtained as a function of  $n_{\text{fit}}$  for  $n_{\text{true}} = 2$  and TBM mixing. All oscillation parameters are kept fixed at their TBM values in the fit for this figure. We reiterate that  $n_{\text{true}}$  is defined as the value of  $n$  for which the  $T_{\text{data}}$  ( $R_{\text{data}}$ ) are generated and  $n_{\text{fit}}$  is the value of  $n$  in  $T_{\text{theory}}$  ( $R_{\text{theory}}$ ). The best fit comes at  $n_{\text{fit}} = 2$ , as expected. We can see that extremely good sensitivity to  $n$  comes for  $\Delta T/T = 5\%$ , while reasonable sensitivity to  $n$  is expected if  $\Delta T/T = 10\%$ . For  $\Delta T/T = 20\%$ , one finds hardly any sensitivity at all, even in this ideal case, where the effect of oscillation parameter uncertainties have been neglected. If  $R$  could be measured at the neutrino telescope, then we expect good sensitivity even if  $\Delta R/R = 30\%$ .

Now we allow the oscillation parameters to vary freely in the fit—the only restriction being that they are not allowed to take values beyond their current  $3\sigma$  limits. We find that, as expected from Fig. 1, there is absolutely no  $n$  sensitivity if  $T$  is used. The reason, as discussed before, is the following: for TBM mixing parameters  $T_{\text{data}} = 1/3$  for  $n_{\text{true}} = 2$ . This value of  $T$  can be reproduced by all values of  $n$ , as long as we are allowed to pick the most suitable set of oscillation parameters which lie within the current  $3\sigma$  limit. Therefore, for this case the  $T_{\text{theory}}$  always exactly reproduces the  $T_{\text{data}}$  and thus  $\chi^2 = 0$  for all  $n_{\text{fit}}$ . For  $R$  the situation is slightly better.  $R_{\text{data}} = 1$  for TBM mixing and  $n_{\text{true}} = 2$ . Hence, as predicted from Fig. 1, values of  $n_{\text{fit}} < 1$  can still be disfavored. The reason being that for  $n_{\text{fit}} < 1$ , it is impossible to get the  $R_{\text{theory}}$  close to 1. However, for  $n_{\text{fit}} > 1$ , one can always find a set of oscillation parameters within the still allowed region which gives the same  $R_{\text{data}}$ . Figure 4 shows the result of the fit.

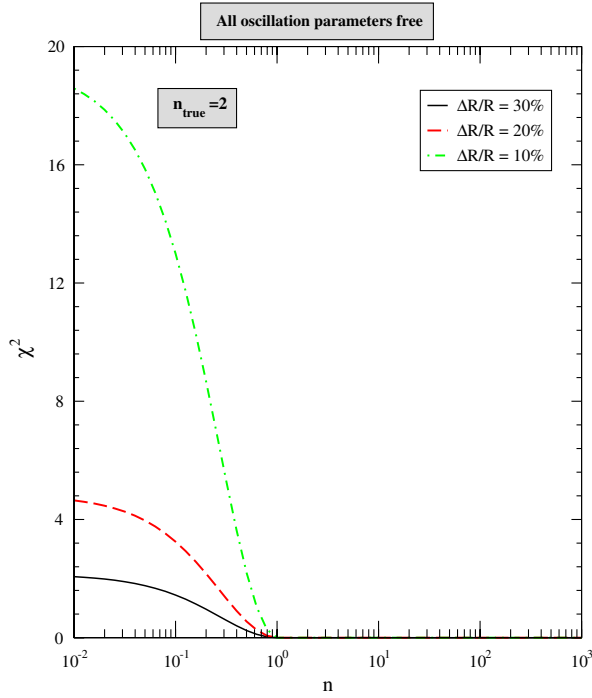


FIG. 4 (color online).  $\chi^2$  as a function of  $n_{\text{fit}}$  for  $n_{\text{true}} = 2$ , for different values of errors on the flux ratios  $R$ . All oscillation parameters are allowed to vary freely within their current  $3\sigma$  limits in the fit. Corresponding  $\chi^2$  for  $T$  is found to be zero for all values of  $n_{\text{fit}}$  and all errors  $\Delta T/T$ .

So far we have shown all  $\chi^2$  sensitivity results assuming that we had  $n_{\text{true}} = 2$ . We next show  $2\sigma$  contour plots in the  $n_{\text{true}} - n_{\text{fit}}$  plane in Figs. 5 and 6. The way these figures are to be interpreted is the following: for each  $n_{\text{true}}$  on the  $x$  axis, the shaded region shows the values of  $n_{\text{fit}}$  which can be excluded at  $2\sigma$ . Figure 5 shows the sensitivity on  $n$  of the neutrino telescope using the more powerful flavor ratio  $R$ , while Fig. 6 gives the corresponding reach by using the more easily measurable  $T$ . The darkest (black) regions are obtained assuming that we have 10% (5%) uncertainty in  $R$  ( $T$ ), the dark (green) regions are for an uncertainty of 20% (10%) in  $R$  ( $T$ ), while the lightest (cyan) regions are for uncertainty of 10% (5%) in  $R$  ( $T$ ). We show these regions in Fig. 5 for the four benchmark sets of mixing parameter cases that we have considered in this paper. The upper left-hand panel is for TBM mixing, the upper right-hand panel is for the EX1 oscillation scenario, the lower left-hand panel is for the EX2 oscillation case, and the lower right-hand for the special case (SPL) of trimaximal mixing in the second row. For  $T$  we show the cases for TBM and EX2 only in Fig. 6. The way we have generated these figures is the following: for each value of  $n_{\text{true}}$  we generate the data for the particular oscillation parameter set. For instance, for the upper left-hand panel of Fig. 5 the data is always generated for the TBM mixing parameters. This data is then fitted with any value of  $n_{\text{fit}}$ , while all oscillation parameters are allowed to vary within their  $3\sigma$  allowed

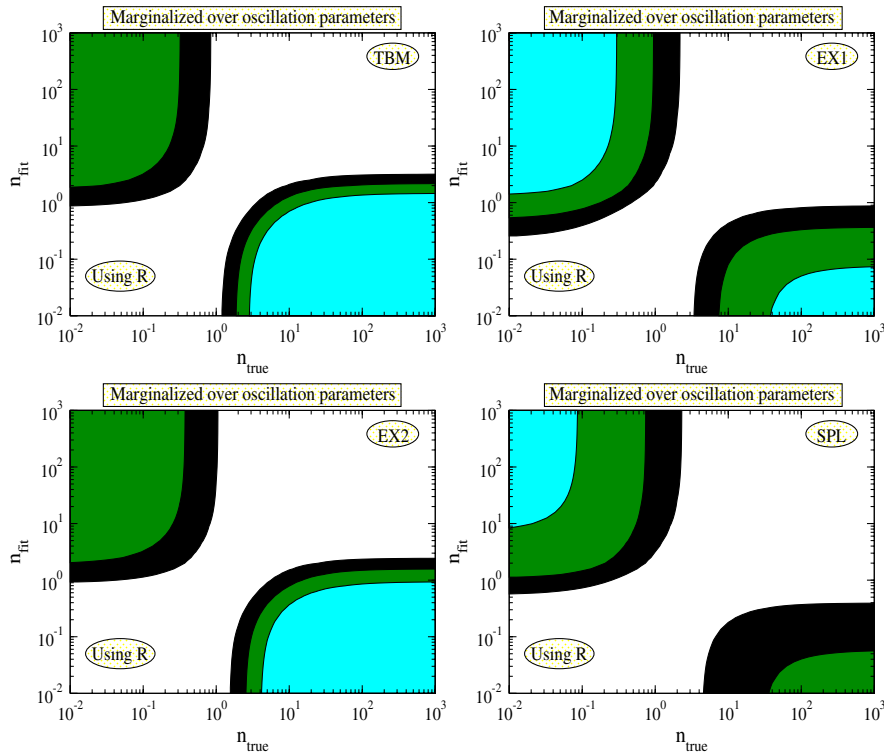


FIG. 5 (color online). For each  $n_{\text{true}}$  on the  $x$  axis, the shaded region shows the values of  $n_{\text{fit}}$  which can be excluded at  $2\sigma$ . We assumed 10% (black/darkest), 20% (green/dark), and 30% (cyan/lightest) uncertainty on  $\Delta R/R$ . The four panels are for the four benchmark values of the oscillation parameters assumed in the data.



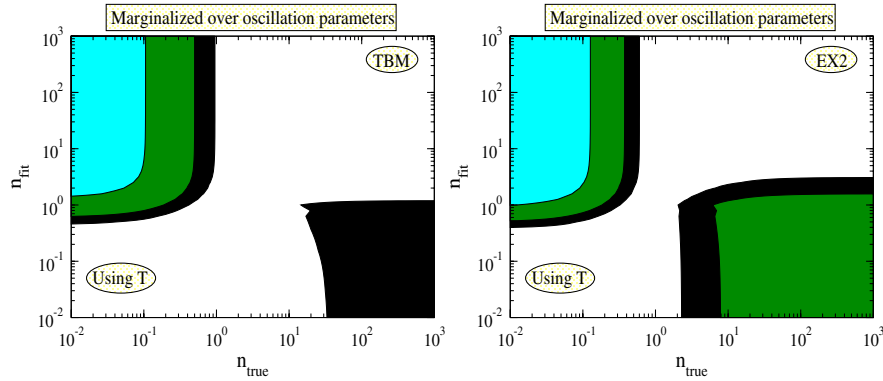


FIG. 6 (color online). For each  $n_{\text{true}}$  on the  $x$  axis, the shaded region shows the values of  $n_{\text{fit}}$  which can be excluded at  $2\sigma$ . We assumed 5% (black/darkest), 10% (green/dark), and 20% (cyan/lightest) uncertainty on  $\Delta T/T$ . The two panels are for the benchmark values TBM and EX2 of the oscillation parameters assumed in the data. Scenarios EX1 and SPL have no sensitivity at all.

range. From Fig. 5 we find that the neutrino telescopes have reasonable sensitivity to the initial flux composition if  $R$  can be measured with reasonable precision. The sensitivity depends sharply on the true value of the oscillation parameters as well as on the true value of  $n$ . We also note that, irrespective of the true oscillation parameter scenario, there is a narrow band around  $n_{\text{true}} \sim 1$ , where we have no sensitivity to the initial flux composition. From Fig. 6 we see that for TBM mixing and EX2,  $T$  returns a sensitivity which is not bad. In particular, for TBM mixing, which is the currently favored scenario, one finds reasonable sensitivity to the flux composition if  $n_{\text{true}} \lesssim 1$ . On the other hand, we have numerically checked that, if the true neutrino mixing turns out to be compatible with the EX1 and SPL case, then it would be almost impossible to determine the UHE neutrino initial flavor composition using  $T$  alone. In other words, there are no shaded regions for SPL and EX1 in the  $n_{\text{true}} - n_{\text{fit}}$  space. This is why we do not show the panels for these cases in Fig. 6.

Of course it is expected that the current uncertainties on the oscillation parameters will decrease [31], as better neutrino oscillation experiments are built and more data is accumulated. This would improve further the prospects of measuring  $n$  at neutrino telescopes.

## VI. CONCLUSIONS AND SUMMARY

Observation of neutrinos with very high energies coming from astrophysical sources has been long overdue. The observed UHE fluxes have a flavor composition on Earth which depends on both their initial composition at source as well as on neutrino flavor oscillations. Therefore, it should be possible to study both kinds of physics with these observations—neutrino physics as well as physics concerning the UHE neutrino sources. Unfortunately, since there are uncertainties in both neutrino mixing parameters as well as knowledge on the type of sources of these UHE neutrinos, attempts on determining one are always plagued by uncertainties on the other.

In this paper we attempted to probe the potential of the future neutrino telescopes in deciphering the flavor composition of the UHE neutrino flux at source. We did this by proposing a very simple and minimal parametrization of the flavor composition at source. We parametrized the initial flux composition of high energy neutrinos simply as

$$(\Phi_e^0 : \Phi_\mu^0 : \Phi_\tau^0) = (1 : n : 0). \quad (31)$$

The parameter  $n$  can take any value from 0 to  $\infty$ . Specific values of  $n$  describe the pure known sources. The UHE neutrino flux depends on a number of astrophysical factors and its exact flavor composition will depend on the process which generates this flux. Neutrinos coming from pion decay will have a flavor ratio of (1:2:0). Likewise a muon-damped source will give a ratio of (0:1:0), a neutron beam source will give (1:0:0), and a charm source (1:1:0). One expects impurities in these relations, i.e., they will not be in the exact form given above. The astrophysical source producing the UHE neutrinos could have a combination of some or all such processes producing these neutrinos. Also, unless there are close-by astrophysical sources, what will be detected at the neutrino telescope is most likely going to be a diffuse flux coming from a combination of different astrophysical sources, and hence it is expected that this observed flux would come as a combination of different neutrino generating decay processes. Since the number of  $\nu_\tau$  produced at the source is negligible, our one parameter description is the most economical and general way of probing the initial flavor composition of the UHE neutrinos.

The observed flavor ratios depend on the neutrino mixing parameters in addition to the property of the source. We studied two of the most used observed flux ratios  $T = \Phi_\mu / (\Phi_e + \Phi_\mu + \Phi_\tau)$  and  $R = \Phi_e / \Phi_\tau$ . We wrote down approximate analytic forms for these flux ratios in terms of  $n$  and the mixing parameters. Using exact numerical results, we showed the uncertainty in  $T$  and  $R$  coming from the current uncertainty on the mixing parameters. It was

shown that the uncertainties due to mixing parameters in minimum around  $n \simeq 1-2$ . We also showed that for both  $T$  and  $R$  the uncertainty due to mixing for small  $n$  was more than that for large  $n$ . We also pointed out a special case where  $T = 1/3$  for all values of  $n$ . This scenario corresponds to the case where the second row of the neutrino mixing matrix has equal entries in all its three elements and illustrates that the ratio  $T$  alone may not suffice to probe  $n$ .

We next defined a simple  $\chi^2$  function and expounded the potential of the neutrino telescopes in determining  $n$  and hence the UHE neutrino flux composition at source. Since the forthcoming neutrino telescopes are yet to collect any data on ultrahigh energy neutrino fluxes, and since it is not yet known what kind of total uncertainty we would have on the observed flux ratios, we performed the  $\chi^2$  analysis for four benchmark points in the mixing parameter space and by assuming different values of errors on  $T$  and  $R$ . Those errors cover assumptions ranging from plausible to optimistic, and allow one to compare the prospects of neutrino telescopes. In particular, our analysis shows what kind of statistics and systematics are required from neutrino telescopes in order to achieve UHE source flavor sensitivity. We first studied the case by assuming a pure pionic source. It was seen that in this case, once the uncertainties due to oscillation parameters were taken into account,  $T$  as measured in neutrino telescopes could give absolutely no information about the flux composition at source. The measured  $R$  could still be used to exclude certain ranges of  $n$  and hence certain types of sources. Finally, we per-

formed a full scan of the  $n$  space, where data was generated at every value of  $n_{\text{true}}$  and the potential of the data to pick the right source  $n$  was studied. We presented  $2\sigma$  contours in the  $n_{\text{true}} - n_{\text{fit}}$  parameter space, which give the  $2\sigma$  initial flux composition sensitivity of the neutrino telescope, as a function of  $n_{\text{true}}$ .

In conclusion, neutrino telescopes will provide information on the flavor composition of the UHE neutrino fluxes on Earth. This can be used to study the initial flavor composition of these fluxes at their source. Reasonable sensitivity to deciphering the correct source flavor composition is expected from these experiments, despite the current uncertainties on the mixing parameters. With projected improvements in our understanding of the neutrino mixing angles, the source flavor sensitivity of the neutrino telescopes will improve.

### ACKNOWLEDGMENTS

We thank Sergio Palomares-Ruiz for helpful comments. W.R. was supported by the ERC under the Starting Grant MANITOP and by the Deutsche Forschungsgemeinschaft in the Sonderforschungsbereich Transregio 27 “Neutrinos and beyond—Weakly interacting particles in Physics, Astrophysics and Cosmology.” S.C. wishes to thank the Max-Planck-Institut für Kernphysik, Heidelberg, where part of this work was completed and acknowledges support from the Neutrino Project under the XI Plan of Harish-Chandra Research Institute.

- 
- [1] J. Ahrens *et al.* (The IceCube Collaboration), Nucl. Phys. Proc. Suppl. **118**, 388 (2003).
  - [2] Information available at <http://www.km3net.org>.
  - [3] S. Pakvasa, Yad. Fiz. **67**, 1179 (2004) [Mod. Phys. Lett. A **19**, 1163 (2004)].
  - [4] P. Bhattacharjee and N. Gupta, arXiv:hep-ph/0501191.
  - [5] P.D. Serpico and M. Kachelriess, Phys. Rev. Lett. **94**, 211102 (2005); P.D. Serpico, Phys. Rev. D **73**, 047301 (2006).
  - [6] Z.Z. Xing and S. Zhou, Phys. Rev. D **74**, 013010 (2006).
  - [7] W. Winter, Phys. Rev. D **74**, 033015 (2006).
  - [8] Z.Z. Xing, Phys. Rev. D **74**, 013009 (2006).
  - [9] M. Kachelriess and R. Tomas, Phys. Rev. D **74**, 063009 (2006); M. Kachelriess, S. Ostapchenko, and R. Tomas, Phys. Rev. D **77**, 023007 (2008).
  - [10] D. Majumdar and A. Ghosal, Phys. Rev. D **75**, 113004 (2007).
  - [11] W. Rodejohann, J. Cosmol. Astropart. Phys. **01** (2007) 029.
  - [12] D. Meloni and T. Ohlsson, Phys. Rev. D **75**, 125017 (2007).
  - [13] P. Lipari, M. Lusignoli, and D. Meloni, Phys. Rev. D **75**, 123005 (2007).
  - [14] R.L. Awasthi and S. Choubey, Phys. Rev. D **76**, 113002 (2007).
  - [15] K. Blum, Y. Nir, and E. Waxman, arXiv:0706.2070.
  - [16] G.R. Hwang and K. Siyeon, Phys. Rev. D **78**, 093008 (2008).
  - [17] S. Pakvasa, W. Rodejohann, and T.J. Weiler, Phys. Rev. Lett. **100**, 111801 (2008).
  - [18] S. Pakvasa, W. Rodejohann, and T.J. Weiler, J. High Energy Phys. **02** (2008) 005.
  - [19] S. Choubey, V. Niro, and W. Rodejohann, Phys. Rev. D **77**, 113006 (2008).
  - [20] A. Esmaili and Y. Farzan, Nucl. Phys. **B821**, 197 (2009); see also K. C. Lai, G. L. Lin, and T. C. Liu, Phys. Rev. D **80**, 103005 (2009).
  - [21] J.F. Beacom, N.F. Bell, D. Hooper, S. Pakvasa, and T.J. Weiler, Phys. Rev. Lett. **90**, 181301 (2003); Phys. Rev. D **69**, 017303 (2004); P. Keranen, J. Maalampi, and J.T. Peltoniemi, Phys. Lett. B **461**, 230 (1999); K. Enqvist, P. Keranen, and J. Maalampi, Phys. Lett. B **438**, 295 (1998); H. Minakata and A.Y. Smirnov, Phys. Rev. D **54**, 3698 (1996); D. Hooper, D. Morgan, and E. Winstanley, Phys. Lett. B **609**, 206 (2005); J.F. Beacom, N.F. Bell, D. Hooper, J.G. Learned, S. Pakvasa, and T.J. Weiler,

- Phys. Rev. Lett. **92**, 011101 (2004); P. Keranen, J. Maalampi, M. Myrskylainen, and J. Riittinen, Phys. Lett. B **574**, 162 (2003); S. Goswami and W. Rodejohann, J. High Energy Phys. 10 (2007) 073; M. Maltoni and W. Winter, J. High Energy Phys. 07 (2008) 064; M. Blennow and D. Meloni, Phys. Rev. D **80**, 065009 (2009).
- [22] S. Pakvasa, Mod. Phys. Lett. A **23**, 1313 (2008).
- [23] G.L. Fogli, E. Lisi, A. Marrone, A. Palazzo, and A. M. Rotunno, Phys. Rev. Lett. **101**, 141801 (2008); M. Maltoni, T. Schwetz, M. A. Tortola, and J. W. F. Valle, New J. Phys. **6**, 122 (2004); A. Bandyopadhyay, S. Choubey, S. Goswami, S. T. Petcov, and D. P. Roy, arXiv:0804.4857.
- [24] J. F. Beacom, N. F. Bell, D. Hooper, S. Pakvasa, and T. J. Weiler, Phys. Rev. D **68**, 093005 (2003); **72**, 019901(E) (2005).
- [25] L. Anchordoqui and F. Halzen, Ann. Phys. (N.Y.) **321**, 2660 (2006).
- [26] J. P. Rachen and P. Meszaros, Phys. Rev. D **58**, 123005 (1998); T. Kashti and E. Waxman, Phys. Rev. Lett. **95**, 181101 (2005).
- [27] L. A. Anchordoqui, H. Goldberg, F. Halzen, and T. J. Weiler, Phys. Lett. B **593**, 42 (2004).
- [28] R. Enberg, M. H. Reno, and I. Sarcevic, Phys. Rev. D **78**, 043005 (2008); **79**, 053006 (2009); R. Gandhi, A. Samanta, and A. Watanabe, J. Cosmol. Astropart. Phys. 09 (2009) 015.
- [29] V. S. Beresinsky and G. T. Zatsepin, Phys. Lett. **28B**, 423 (1969); R. Engel, D. Seckel, and T. Stanev, Phys. Rev. D **64**, 093010 (2001).
- [30] J. D. Bjorken, P. F. Harrison, and W. G. Scott, Phys. Rev. D **74**, 073012 (2006); X. G. He and A. Zee, Phys. Lett. B **645**, 427 (2007); C. S. Lam, Phys. Rev. D **74**, 113004 (2006); W. Grimus and L. Lavoura, J. High Energy Phys. 09 (2008) 106; Phys. Lett. B **671**, 456 (2009); C. H. Albright and W. Rodejohann, Eur. Phys. J. C **62**, 599 (2009); C. S. Lam, arXiv:0907.2206.
- [31] A. Bandyopadhyay *et al.* (ISS Physics Working Group), Rep. Prog. Phys. **72**, 106201 (2009); P. Huber, M. Lindner, T. Schwetz, and W. Winter, J. High Energy Phys. 11 (2009) 044; A. Bandyopadhyay, S. Choubey, S. Goswami, and S. T. Petcov, Phys. Rev. D **72**, 033013 (2005).